A Study of Volatiles Emitted During Bio-Oil Upgrading to Bio-Pitch

Simon Laliberté-Riverin[1], Marie Aimée Tuyizere Flora[2] and Houshang Alamdari[3]
1. Postdoctoral Fellow
2. Ph. D. Student
3. Professor
Aluminium Research Center, REGAL, Department of Mining, Metallurgical and Materials Engineering, Laval University, Quebec, Canada
Corresponding author: simon.laliberte-riverin@gmn.ulaval.ca
https://doi.org/10.71659/icsoba2025-el004

Abstract

Replacing coal-tar pitch in carbon anodes with a binder derived from biomass is an active research topic. The development of such a binder, known as bio-pitch, could help the aluminium industry in reducing its carbon footprint. However, this technology has not yet been demonstrated on an industrial scale. Bio-pitch is produced through the upgrading of wood pyrolysis oil (bio-oil), either by heat treatment or distillation. More knowledge about the mechanisms of bio-oil upgrading is required to produce binders that meet industrial requirements. In this work, we analyzed the volatiles evolved during the heat-treatment of bio-oil up to 250 °C. The temperature, mass loss, and composition of the volatiles were monitored simultaneously using a thermogravimetric analysis setup coupled with a quadrupole mass spectrometer. Time series data was collected on ion abundance for mass-to-charge ratios of 1–150. The data was deconvoluted using principal component analysis, to reconstruct the mass spectra of desorbed species and link them with their emission profiles. It was found that a group of water-rich compounds, containing acids and oxygenates, starts vaporizing around 100 °C, and that another group of compounds containing heavier molecules can be detected after reaching 150 °C. This information could be used to fine-tune bio-oil heat-treatment processes.

Keywords: Carbon anodes, Bio-pitch, Mass spectrometry, Thermogravimetric analysis, Principal component analysis.

1. Introduction

The term “bio-pitch” designates a solid, thermoplastic material, originating from the pyrolysis of biomass. It is usually obtained after upgrading of the pyrolytic oil, or “bio-oil”, which is, along with biochar and biogas, a coproduct of biomass pyrolysis [1]. There has been interest in recent years into considering bio-pitch as a potential substitute for coal-tar pitch in pre-baked anodes [2]. Such a substitution could potentially reduce the fossil CO_2 emissions associated with coal-tar pitch production, anode baking and carbon consumption in electrolysis cells [3]. However, this technology is not currently ready for industrial production.

Reports about lab-scale anodes made with bio-pitch state a baked apparent density similar [4] or slightly inferior [5] to that of coal-tar pitch-based anodes, similar electrical resistivity [4], and slightly higher air and CO_2 reactivities [4]. Bio-pitch contains oxygenated compounds which make its chemical composition much different from that of coal-tar pitch, the latter containing mainly heterocyclic and polycyclic aromatic hydrocarbons [6]. The presence of oxygenated compounds in bio-binders hinders mesophase formation, causing the baked microstructure to be isotropic with a low L_c [4, 7]. In addition, the oxygenated compounds are volatilized during baking, leaving behind a low fixed carbon content or low coking value product [4].

Anode paste needs to be mixed and formed at a temperature higher than the softening point of the binder, but the binder needs to solidify at room temperature to facilitate handling of the anodes. Upgrading of bio-oil to bio-pitch is done to remove water and relatively light compounds and give the binder the desired thermoplastic properties. Upgrading can be done by heat treatment [4, 7], vacuum distillation [8], or flash distillation [9]. The upgrading conditions, mainly time and temperature, control the softening point, the coking value and the viscosity of the binder as well as its wettability to calcined petroleum coke. However, these properties are interrelated and difficult to tune independently [8].

The optimal temperatures reported for bio-oil upgrading are close to 180 °C. Ideally, a higher heat-treatment temperature would be needed to increase the coking value, but a higher temperature causes cross-linking of oxygenated functional groups, and a corresponding increase of viscosity and loss of thermoplastic properties and wettability to coke [10]. A more detailed understanding of heat-treatment kinetics could help to fine-tune the heat-treatment conditions and ultimately obtain better quality binders.

In this work, a bio-oil sample is put in a reactor and subjected to simulated heat-treatment conditions. The mass loss is monitored continuously with an analytical balance, while the evolved volatiles are analyzed with an online quadrupole mass spectrometer. Deconvolution of the time evolution of mass spectrometry data with principal component analysis reveals insights on the volatile evolution kinetics.

2. Materials and Methods

2.1 Bio-Oil

The bio-oil used in this work was produced by vacuum pyrolysis [11] of spruce wood chips (Pyrovac, Saint-Lambert-de-Lauzon, Québec, Canada). The bio-oil has a water content of 18 wt.% and an oxygen level of 30.5 wt.% (dry basis) [12].

2.2 Test Setup and Test Conditions

The reactor, Figure 1, comprises a vertical steel cylinder inside a vertical tube furnace (3210 Series, Applied Test Systems, Butler, PA, USA). The top of the cylinder is closed by a blind flange which contains two type K thermocouples and an open hole. On top of the setup, there is a box in which the volatiles coming out of the hole in the top flange are extracted. A balance with a precision of ±0.01 g (Model ML802T, Mettler-Toledo, Greifensee, Switzerland) is placed on top of the box. The sample (8 g) is put in a glass test tube in a wire mesh basket suspended on a hook under the balance via a steel rod that passes through the hole in the top flange of the cylinder. The weight is recorded continuously on a computer through a USB connection.

A connection on the side of the vertical steel cylinder is used as a continuous sampling point. The sample is brought to the spectrometer via a capillary transfer line, heated to 300 °C to prevent volatile condensation throughout the process. The sample is analyzed at 30 s intervals for mass-to-charge ratios (m/z) between 1 and 150 with a quadrupole mass spectrometer (Calypso DS, In Process Instruments, Bremen, Germany). The spectrometer is equipped with an electron impact ion source, a Faraday cup and an electron multiplier. Air or argon is injected through a connection at the bottom of the cylinder and is controlled to 5 L/min with a mass flow controller (SLA5850S, Brooks Instruments, PA, USA). It should be mentioned that the upgrading of bio-oil to bio-pitch is normally done in air. The tests in Ar were done to determine if there was any reaction between air and bio-oil.

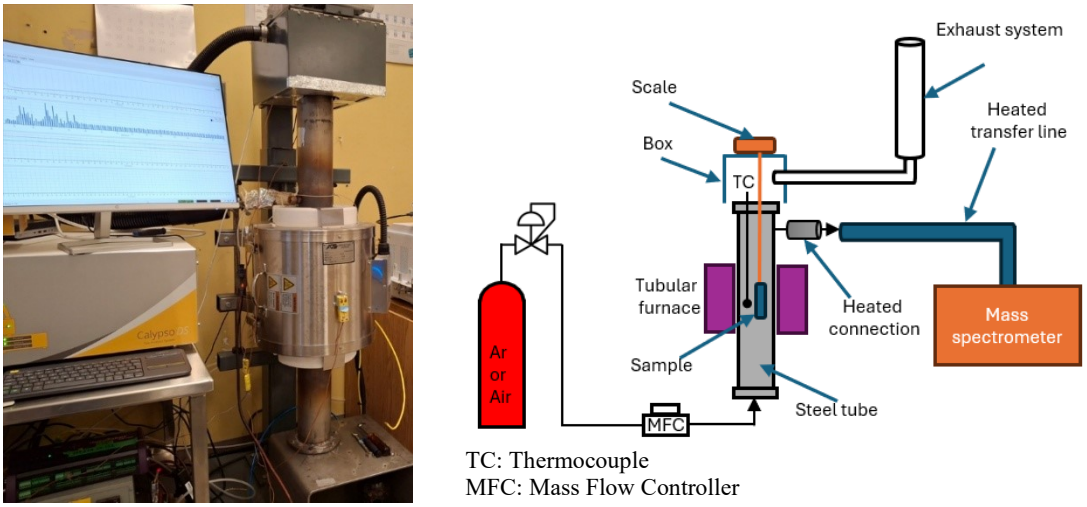

TC: Thermocouple
MFC: Mass Flow Controller

Figure 1. Left: Picture of the furnace and mass spectrometer. Right: Schematic of setup.

For each test, the sample was left at room temperature in the chosen atmosphere for 30 min. The furnace was then heated at a constant heating rate until reaching the setpoint and left for a soaking time of 1 h. The heating rates and maximum temperatures varied slightly, Table 1, possibly due to differences in specific heat or heat transfer coefficients between gases. One mass spectroscopy data baseline was produced for each condition, without a sample. Tests were duplicated.

Table 1. Experimental conditions.

Description	Sample mass (g)	Heating rate (°C/h)	Maximum temp. (°C)
Air, baseline	–	69.4	229.0
Air, sample #1	8.51	71.3	234.0
Air, sample #2	7.90	65.4	222.0
Argon, baseline	–	66.3	243.4
Argon, sample #1	7.84	72.9	241.0
Argon, sample #2	8.08	67.3	245.5

2.3 Data Treatment

The data from the balance and thermocouples were recorded on one computer, and mass spectrometry data on a separate computer. The data were time-synchronized and then merged into one dataset. Since the original data from the balance and thermocouples were recorded every 5 s and the data from mass spectrometry every 30 s, the sample mass and temperature data were resampled on the same time coordinates as the mass spectrometry data by forward filling. The balance and thermocouple signals were filtered with a Savitzky-Golay filter [13] to reduce the noise. The thermogravimetric (TG) data was taken as the ratio of mass loss over the initial mass; and the time derivative of this signal was taken as the mass loss rate (DTG) signal.

Time-based mass spectrometry gives high dimensionality data – in this case, 150 channels with a high degree of correlation between the channels. One type of evolved molecule can generate signals on several mass channels simultaneously as per its electron impact fragmentation pattern [14]. A suitable method to reduce the dimensionality is principal component analysis (PCA), which decomposes the signal in orthogonal, independent signals, aiming to explain the maximum of variance [15]. This strategy has been applied successfully for time-based mass spectrometry data [16]. In the present paper, the widely available Scikit-learn Python package was used to perform the PCA. The mass channel and DTG data are normalized first using the *MinMaxScaler* and then transformed into three principal components using a *SparsePCA* [15].

From the PCA analysis, the following are obtained 1) the time and temperature evolution of the principal components (PC's), and 2) the unit vectors, which are the normalized intensities of each mass channel for each PC. These normalized intensities are then multiplied by the individual peak intensities (i.e. the difference between the maximum and the minimum current during the whole measurement period) to give tentative mass spectra associated with each PC.

3. Results

3.1 Thermogravimetric Analysis

The reconciliation between the weighing of the sample before and after the test and the mass loss measured in the TGA setup is shown in Table 2. The measurement in the TGA setup is stopped after the isothermal segment, thus neglecting further mass loss during cooling down. However, the difference between the two measurements in air is negligible. The mass loss in argon seems to be slightly higher than in air. No TGA results are available for samples tested in argon. More details on the tests with argon are given in Section 3.5.

Table 2. Mass loss during test.

Test #	Initial sample mass (g)	Final sample mass (g)	Mass loss per weighing (%)	Mass loss per TGA (%)
Air #1	8.51	4.61	45.8	45.0
Air #2	7.90	4.17	47.2	47.0
Argon #1	7.84	3.97	49.4	–
Argon #2	8.08	4.14	48.8	–

Figure 2 shows the DTG data in the ramp segment for the two samples tested in air. For both samples, the mass loss increases gradually after 50 °C, and then steeply after 130 °C, before reaching a peak between 170 °C and 200 °C and slowly decreasing past the peak. The blue curve (Air #1) is a bit offset to higher temperatures, with the red curve having a higher mass loss rate for a given temperature during the heating phase. This may be due to the slightly higher heating rate of the Air #1 sample.

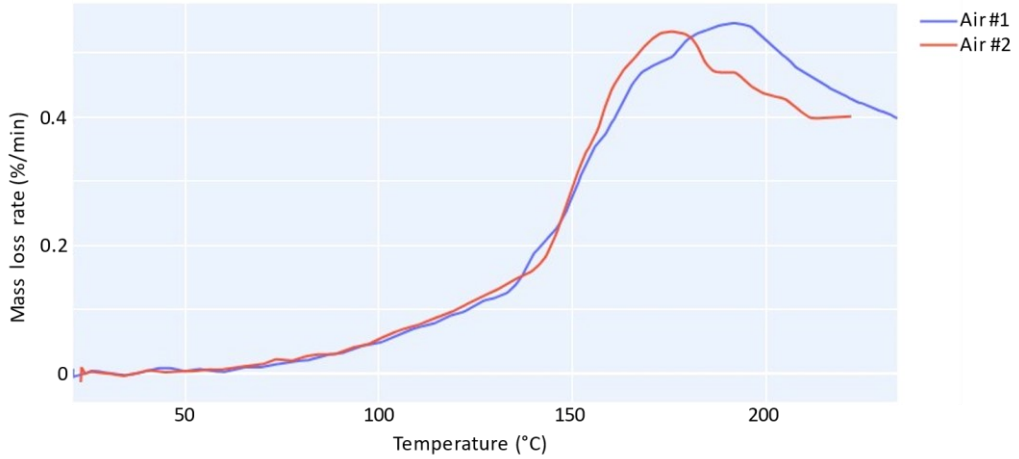

Figure 2. DTG data for bio-oil samples tested in air.

3.2 Mass Spectra

Mass spectra from sample Air #1 at 50 °C and 200 °C are shown in Figure 3. Since the sample Air #1 and Air #2 results were similar, only sample Air #1 results are shown from this point on.

At 50 °C, the most prominent peaks are N_2 (m/z 28 and 14), O_2 (32 and 16), Ar (40) and CO_2 (44), which are all from the air atmosphere inside the furnace. The Ar and CO_2 signals are from background levels in the air. At 200 °C, other peaks are also visible: 18, 43, 45, 60.

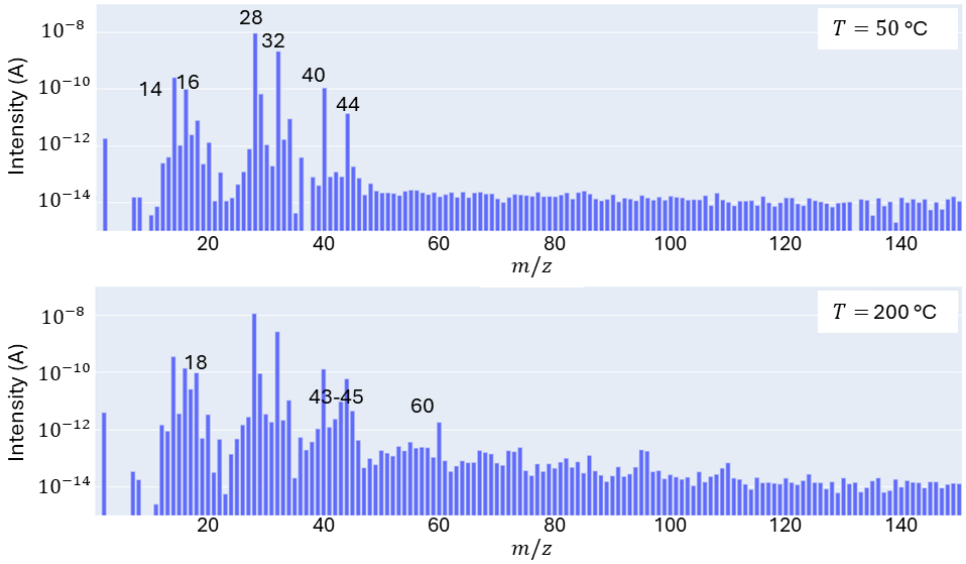

Figure 3. Instantaneous mass spectra for sample Air #1, taken at different temperatures.

Figure 4 shows data from some individual mass channels as a function of temperature during the heating stage of the experiment. The blue curve is the signal from the sample, and the gray one is the baseline. Some signals (m/z 18, 43, 60), start deviating from the baseline between 80 °C and 120 °C, peak between 200 °C and 220 °C, and then start decreasing at higher temperatures. This behavior is common to other channels not shown in Figure 4 (m/z 17, 19, 31, 45, 59, 72, 74). Other signals (m/z 40, 44, 96), increase monotonically when the temperature is raised. Those corresponding to permanent gases (m/z 28, 32, 40, 44) deviate from the baseline around 100 °C, and others (m/z 96 shown in Figure 4, m/z 12, 26, 27, 37, 39) start increasing around 150 °C.

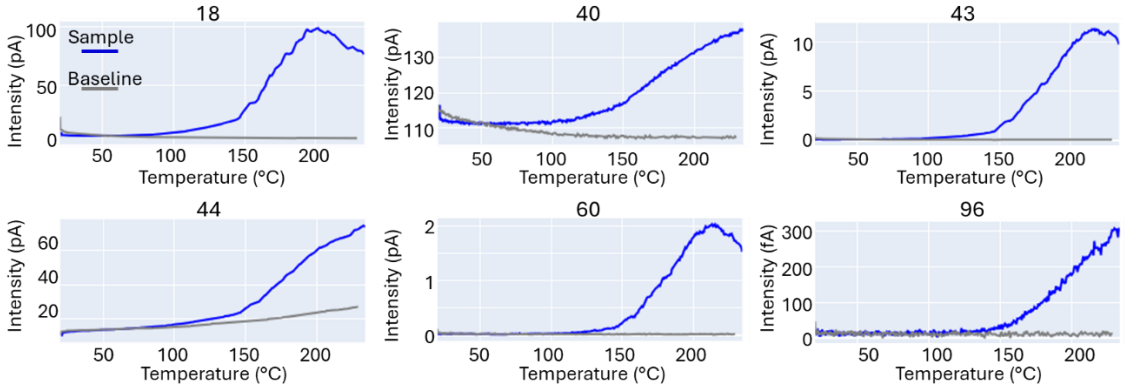

Figure 4. Intensity of mass signal as a function of temperature. m/z shown on top of graphs.

Time-based data (Figure 5), further distinguishes between two types of behavior. For the channels corresponding to the permanent gases, the monotonically increasing signal during the heating segment (green marker) becomes constant during the soaking time (yellow marker). For the other signals, an exponential-like decay is observed once the isothermal section is reached.

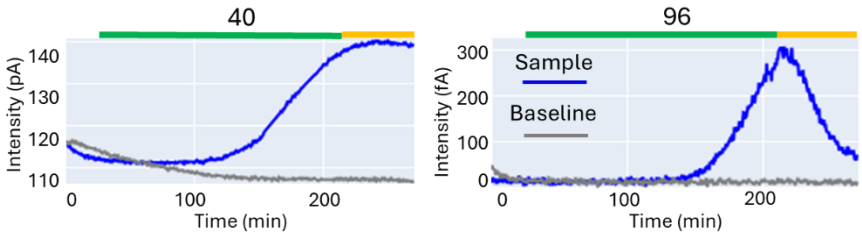

Figure 5. Intensity of mass signal as a function of time. m/z shown on top of graphs. Green bar: heating segment; yellow bar: isothermal segment.

3.3 Decomposition of Mass Spectrometry Data in Principal Components

It was found that the optimal number of principal components (PC) was three, and if more were used, they contained only random noise. The evolution of the three PC's as a function of temperature and time are shown in Figure 6. The three distinct behaviors observed on individual mass channels are captured by the PCA. The PC1 intensity increases with temperature during ramp-up and decreases exponentially during the isothermal segment. PC2 shows a peak during the ramp-up segment and also decreases exponentially during the isothermal segment. Finally, PC3 shows a monotonic increase during the ramp-up segment and stabilization during the isothermal segment.

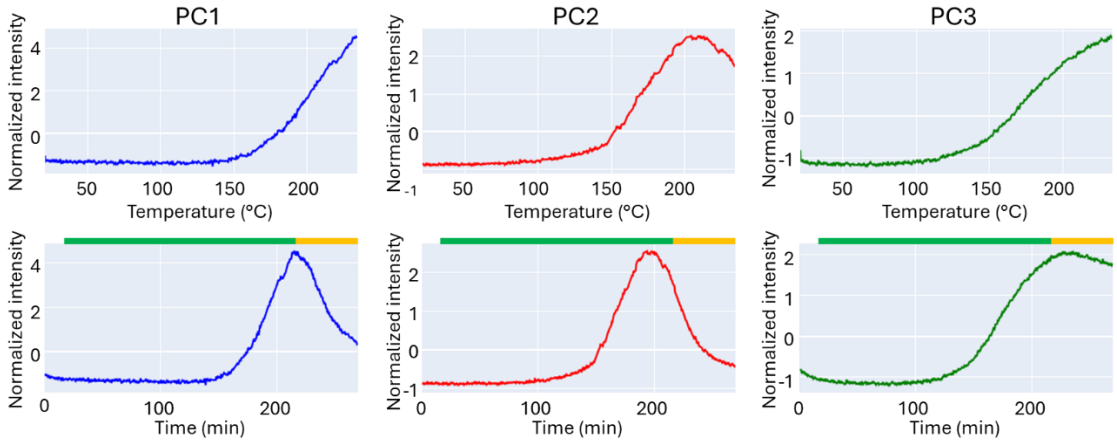

Figure 6. Temperature (top) and time (bottom) evolution of the three PC's. Green bar: heating segment; yellow bar: isothermal segment.

Figure 7 shows the denormalized vectors, obtained by the elementwise product of the unit vectors associated with each PC by the maximum peak intensity in each channel. The unit vectors for each PC and channel contain a value that can be seen as a quantitative indication of the adherence of the data of the channel to the behavior of the PC shown in Figure 6. By multiplying each of these values by the intensity of the original data (maximum minus minimum of signal in each mass channel), we reconstitute a tentative mass spectrum to help identify the species constituting each PC. In other words, we assume that those three PC's exhibiting distinct behavior correspond to three groups of compounds that are detected at different times and temperatures, and we use the denormalized vectors to identify them.

The use of spectrometric database search functions to perform identification of components from those spectra is not feasible, because 1) each PC contains several compounds, and 2) the ratios of intensities are likely different from the database data because the methods for obtaining them

differ in the present work. As an alternative, a list of plausible compounds was established and then narrowed down by correlating their properties and main peaks with experimental data.

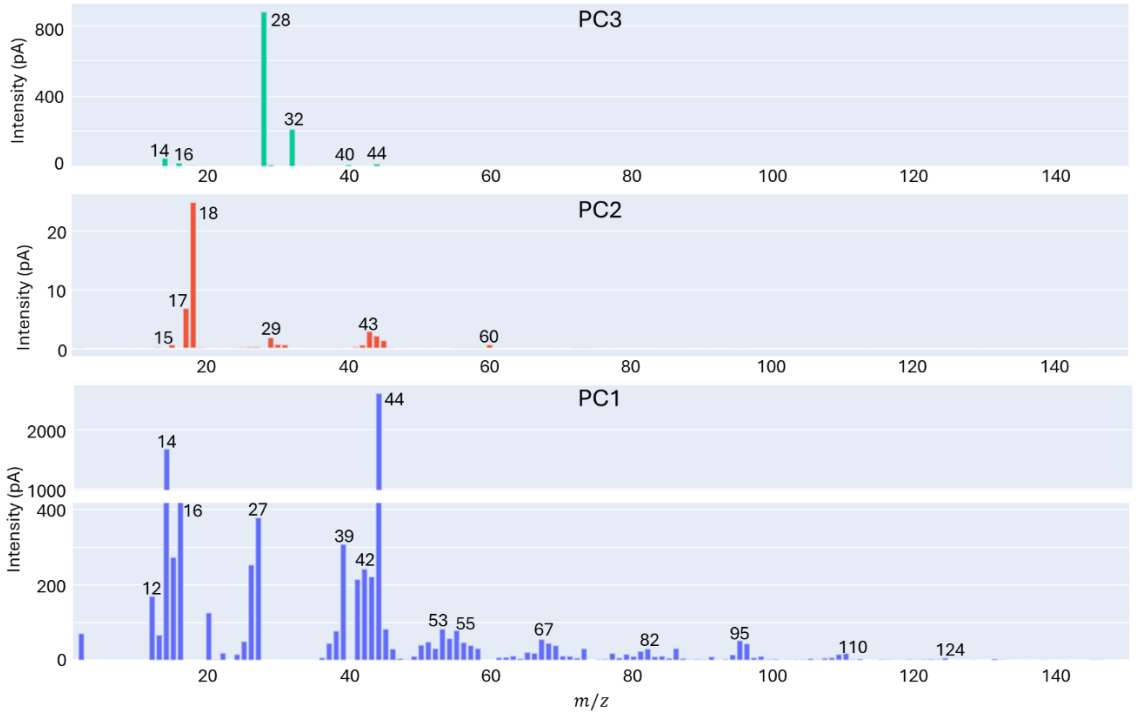

Figure 7. Denormalized vectors associated with each PC.

The list of candidate compounds, Table 3, was established from a round-robin study on the analysis of bio-oils [18]. The molecular weight (m_w), boiling point (T_b) and list of peaks [17] were added to the table. The peaks shown in bold in the table have intensities larger than 50 % of the largest peak, according to electron impact fragmentation data [17], while peaks with an intensity smaller than 10 % of the largest peak are not shown. The blue, red and green colors in Table 3 correspond to compounds primarily detected in PC1, PC2 and PC3, respectively.

Table 3. Selected candidate compounds and their properties [17].

Compound	Formula	m_w (g/mol)	T_b (°C)	Main peaks (m/z)
Nitrogen	N_2	28.013	-195.9	**28**, 14
Oxygen	O_2	31.999	-183.0	**32**, 16
Argon	Ar	39.948	-185.7	**40**, 20
Carbon dioxide	CO_2	44.010	-78.5	**44**, 12, 16, 28
Water vapor	H_2O	18.015	100.0	**18**, 17
Formic acid	CH_2O_2	46.025	100.8	**29, 46, 45,** 17, 28, 44
Acetic acid	$C_2H_4O_2$	60.052	118.1	**43, 45, 60**, 15, 42, 29
Hydroxy-acetaldehyde	$C_2H_4O_2$	60.052	97.0	**31, 32**, 29, 28
Acetol	$C_3H_6O_2$	74.079	145.6	**43**, 31, 15, 74
Propionic acid	$C_3H_6O_2$	74.079	140.9	**74, 28, 45, 29, 27, 73,** 57, 55, 56, 26
Butyric acid	$C_4H_8O_2$	88.105	162.9	**60, 73,** 41, 27, 42, 43, 45
Furfural	$C_5H_4O_2$	96.084	161.6	**96, 95, 39**, 38, 29, 37, 67
Guaiacol	$C_7H_8O_2$	124.13	205.1	**109, 124, 81**, 53, 52, 51, 39, 27
Cresol	C_7H_8O	108.13	191.2	**108, 107**, 79, 77, 90, 39, 51, 80

The first and most evident association can be made between PC3 and the permanent gases (N_2, O_2, Ar and CO_2). This is demonstrated by the presence of the peaks specific to those gases (m/z 28, 32, 40, 44, 14, 16) in Figure 7, and by the correlation between the time evolution of PC3 and that of the signals on those channels. The reason for the increase in intensity of those signals with temperature is not known, however.

For PC2, the most prominent peak in the denormalized vector is for an m/z of 18 (H_2O^+), followed by 17 (OH^+) which indicates the presence of an aqueous phase. Significant peaks are also observable at m/z 29, 43, 44, 45 and 60, which are associated with carboxylic acids, such as formic, acetic, or propionic acids, which would co-evaporate with water. Peak m/z 60, corresponds to the molecular ion (M^+) from acetic acid or an ion fragment obtained from higher molar mass carboxylic acids [14]. Peak 45 corresponds to $COOH^+$ from any carboxylic acid; and peak 43 to the M–OH^+ ion from acetic acid. The presence of the m/z peak 74 could also be an indication of the presence of acetol, which is reported to be present in bio-oils [18].

The denormalized vector of PC1 contains many peaks, making the task of identification more complicated. However, by cross-referencing the most prominent peaks in the high mass range ($\boldsymbol{m/z}$ 95, 110, 124) with mass spectrometry data from the typical bio-oil compounds in Ref. [18] which have a boiling point commensurate with the test temperature, we identified three possible compounds constituting this PC: furfural, guaiacol and cresol.

Figure 8 shows a reconstruction of the original data by a weighted sum of the three PC's with the unit vectors used as weights. In the figure, the original, normalized data is shown in black. Each product of PC × (unit vector intensity) is shown as blue, red, or green (same color code used before). The sum is shown as a gray curve, labeled "regression". For channels strongly associated with one of the three PC's, the reconstructed curve fits well with the original data (m/z 18, 28 and 110).

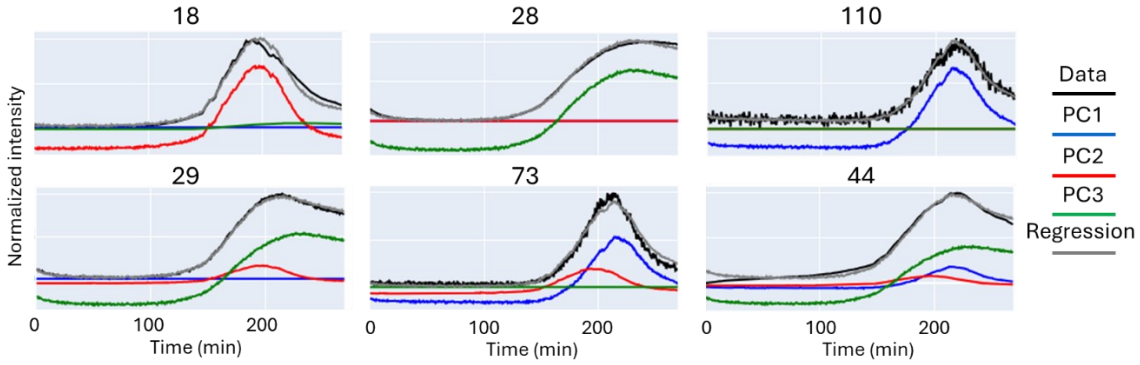

Figure 8. Reconstruction of normalized data by summation of PC's.

For some cases, more than one PC can be visible on the same mass channel. For instance, in the case of m/z 29, this peak appears in several compounds of PC2 in Table 3, but it can also appear in N_2, due to the natural occurrence of isotope ^{15}N. Propionic and butyric acids both share the peak m/z 73, but due to its higher boiling point, it is possible that butyric acid co-evaporates with the compounds in PC1, as hinted by the presence of both the blue and red PC's in the reconstructed spectrum of Figure 8. The m/z 44 graph shows the presence of the three PC's. This peak is the main peak on CO_2 mass spectra. Fragments with a m/z 44 are also present in several compounds, but in small intensity (hence not shown in Table 3). These weak fragments would not account for the high m/z 44 peak in PC1. A possible explanation for the presence of a m/z 44 peak in PC1 is the in-situ generation of CO_2 by decarboxylation or decarbonylation of bio-oil compounds [19].

3.4 Reconstruction of the Thermogravimetric Data

The DTG signal (mass-loss rate) was also included in the PCA analysis and reconstructed according to the same method as described in the last section, Figure 9. At first glance, the mass loss rate seems correlated only with PC2, which would mean that the mass loss is only from the aqueous phase. However, there is a shift to the left of the DTG signal compared to the mass spectrometry data. This is possibly due to the time lag between the volatile emission, which is recorded immediately by the balance, and its detection in the MS. For this reason, the time lag should be estimated and compensated before doing the PCA, which is outside the scope of this paper. Therefore, this data should be viewed cautiously. Nevertheless, in future experiments, if the DTG data was successfully deconvoluted into separate PC's, it would enable estimating the contribution of each of the group of compounds on the mass of the volatiles emitted.

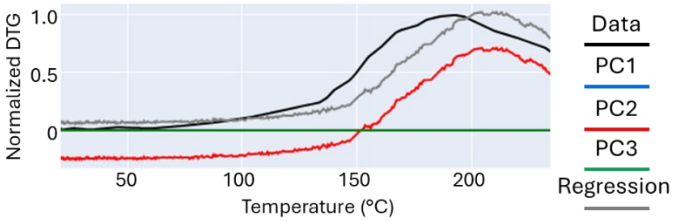

Figure 9. Reconstruction of DTG data

3.5 Tests in Ar Atmosphere

Tests were also performed with the injection of Ar. However, the maximum achievable concentration of Ar in the reactor was 85 %, with residual O_2 levels around 3 %. The reactor is not leak-tight because of the hole in the top flange which allows the passage of the rod attached to the balance. A higher flow of Ar in the system would be needed to keep lower O_2 levels, but it is not achievable with the current system. Nevertheless, the tests done in Ar atmosphere (or more accurately, low O_2 atmosphere) are not shown, because they were similar to the results in air, except for PC3, which had higher intensities for peaks m/z 20 and 40 (Ar^{2+} and Ar^{+}) and relatively lower intensities for the peaks corresponding to the other permanent gases. The similarity of results in oxygen-rich and oxygen-poor atmospheres are in accordance with the literature; it was shown that pyrolysis and low-temperature oxidation of bio-oils below 300 °C are both characterized by removal of water and oxygenated compounds from the liquid phase and do not exhibit significant differences in terms of mass loss and composition of volatiles [19].

4. Discussion

The analysis above reveals insights that can be useful in an industrial perspective. To reach desirable properties, a binder must have a high fixed carbon content (i.e. coking value) and a low oxygen content, to prevent undesirable cross-linking and loss of thermoplastic properties. A plausible strategy to optimize the properties of the bio-pitch would be to fine-tune the conditions of the heat-treatment during bio-oil upgrading to bio-pitch in order to maximize the carbon and minimize the oxygen content. It can be seen from Table 3 that the organic compounds identified as part of PC2 contain two oxygen atoms and up to three carbon atoms, so their oxygen mass percentage varies between 43 % and 70 %, and their carbon percentage between 25 % and 50 %. In contrast, for PC1, which contains between 4 and 7 carbon atoms for two oxygen atoms, the oxygen mass percentage varies between 15 % and 36 %, and the carbon content between 55 % and 78 %. Therefore, on an industrial standpoint it would be beneficial to evaporate the compounds in PC2 as much as possible, while keeping the compounds in PC1 in the binder. Since it was observed that the two groups of compounds do not evolve at the same temperature, one

could potentially achieve this by fine-tuning the heat-treatment conditions, for example by modulating the heating rate or adding isothermal steps. The results also did not show a significant effect of the amount of oxygen in the atmosphere on the kinetics of heat-treatment, hinting that conducting the heat-treatment in air is a sound approach. Nevertheless, the results shown in this work are qualitative. It was not possible to determine the mass lost with each of the groups of compounds. More detailed studies would be required to further improve the heat-treatment conditions.

5. Conclusions

In the present work, we used a coupled thermogravimetric–mass spectrometric setup to study the volatiles emitted during the heat-treatment of bio-oil to bio-pitch. It was shown that two groups of compounds are volatilized at different temperatures during the heat-treatment of bio-oil to bio-pitch. The first group is rich in water, acids and other oxygenated compounds with molar mass < 75 g/mol and boiling points of 100 °C to 150 °C (PC2). It starts evaporating around 100 °C, and evaporation peaks around 200 °C. The second group (PC1) contains heavier oxygenated compounds (> 75 g/mol) with boiling points higher than 160 °C. Vaporization of those compounds starts around 150 °C, and most likely peaks slightly higher than the maximum test temperature.

The presence of oxygen in bio-binders has undesirable effects, such as limiting the achievable coking value of the binder. Since the compounds in PC2 have higher oxygen content than those in PC1, a possible strategy to improve the quality of binders would be to design new heat-treatments to maximize the removal of oxygen in PC2, while keeping as much carbon as possible in the binder, by minimizing volatilization of PC1. The methodology proposed in this paper can help these further developments by monitoring the vaporized species in a high level of detail.

6. Acknowledgements

This project was funded by Alcoa and the Natural Sciences and Engineering Research Council of Canada, NSERC (Alliance-Avantage-2020-557053). Part of the research presented in this work was financed by the Fonds de recherche du Québec – Nature et technologies, through the Aluminium Research Centre – REGAL (FRQNT-2024-RSMA-340932). S. Laliberté-Riverin thanks the Fonds de recherche du Québec for the postdoctoral fellowship (FRQNT-B3-357820, https://doi.org/10.69777/357820). The mass spectrometer used in this work was provided by InProcess Instruments and Isomass Scientific Inc. The bio-oil was provided by Pyrovac inc.

7. References

1. Anthony V. Bridgwater, Review of fast pyrolysis of biomass and product upgrading, Biomass and Bioenergy, Vol. 38, 2012, 68–94. https://doi.org/10.1016/j.biombioe.2011.01.048
2. Samuel Senanu and Asbjørn Solheim, Biocarbon in the Aluminium Industry: A Review, Light Metals 2021, 649–656. https://doi.org/10.1007/978-3-030-65396-5_87
3. Bernard Osei, Simon Laliberté-Riverin, and Houshang Alamdari, A Cradle-to-Gate Life Cycle Assessment of Pre-baked Carbon Anode Production; A Case Study in Quebec, Proceedings of the 42nd International ICSOBA Conference, Lyon, Oct. 2024, TRAVAUX 53, 807–829.
4. Asem Hussein, Donald Picard, and Houshang Alamdari, Biopitch as a Binder for Carbon Anodes: Impact on Carbon Anode Properties, ACS Sustainable Chemistry & Engineering, Vol. 9, No. 12, (2021), 4681–4687. https://doi.org/10.1021/acssuschemeng.1c00618

5. Nooshin Baastani et al., Effect of Mixing and Pressing Parameters on the Properties of Biopitch-Based Lab-Scale Carbon Anodes for Use in the Hall-Héroult Electrolytic Cell, Light Metals 2024, 804–814. https://doi.org/10.1007/978-3-031-50308-5_101
6. André Charette et al., Experimental and kinetic study of volatile evolution from impregnated electrodes, Fuel, Vol. 69, No. 2, (1990), 194–202. https://doi.org/10.1016/0016-2361(90)90173-N
7. Gøril Jahrsengene et al., Bio-Binders and Their Carbonization and Interaction with Petroleum Coke During Baking, Light Metals 2022, 883–889. https://doi.org/10.1007/978-3-030-92529-1_116
8. Ying Lu et al., Synthesis and Characterization of Bio-pitch from Bio-oil, ACS Sustainable Chemistry & Engineering, Vol. 8, No. 31, (2020), 11772–11782. https://doi.org/10.1021/acssuschemeng.0c03903
9. Yaseen Elkasabi et al., Flash Distillation of Bio-Oils for Simultaneous Production of Hydrocarbons and Green Coke, Industrial & Engineering Chemistry Research, Vol. 58, No. 5, (2019), 1794–1802. https://doi.org/10.1021/acs.iecr.8b04556
10. Ying Lu et al., Properties of Bio-pitch and Its Wettability on Coke, ACS Sustainable Chemistry & Engineering, Vol. 8, No. 40, (2020), 15366–15374. https://doi.org/10.1021/acssuschemeng.0c06048
11. Christian Roy, D. Morin, and F. Dubé, The biomass Pyrocycling process, Proceedings of the International Conference on Gasification and Pyrolysis of Biomass, Stuttgart, 1997, 9–11.
12. Marie Aimee Tuyizere Flora et al., Bio-pitch improvement for coal-tar pitch replacement in pre-baked anodes, Proceedings of the 41st International ICSOBA Conference, Dubaï, Oct. 2023, TRAVAUX 52, 1047–1059.
13. The SciPy Community, SciPy documentation. Accessed: Apr. 28, 2025. [Online]. Available: https://docs.scipy.org/doc/scipy/index.html
14. James M. Thompson, Mass Spectrometry. Pan Stanford Publishing Pte. Ltd., 2018. https://doi.org/10.1201/9781351207157
15. Scikit-learn, User Guide, https://scikit-learn.org/stable/user_guide.html (Accessed on 29 April 2025).
16. Tobias M. Richter et al., Evaluation of PTR-ToF-MS as a tool to track the behavior of hop-derived compounds during the fermentation of beer, Food Research International, Vol. 111, (2018), 582–589. https://doi.org/10.1016/j.foodres.2018.05.056
17. NIST, NIST Chemistry Webbook, SRD69, https://doi.org/10.18434/T4D303. (Accessed on 29 April 2025).
18. Anja Oasmaa and Dietrich Meier, Pyrolysis liquids analyses - The results of IEA-EU round robin, Fast Pyrolysis of Biomass: A Handbook, Vol. 2, CPL Press, 2002, 41–58.
19. Javier Ordonez-Loza et al., An investigation into the pyrolysis and oxidation of bio-oil from sugarcane bagasse: Kinetics and evolved gases using TGA-FTIR, Journal of Environmental Chemical Engineering, Vol. 9, No. 5, (2021), 106144. https://doi.org/10.1016/j.jece.2021.106144